This is an open access article published under a Creative Commons Attribution (CC-BY) License, which permits unrestricted use, distribution and reproduction in any medium, provided the author and source are cited.

ACS OMEGA

http://pubs.acs.org/journal/acsodf

Article

Glutathione Surface Molecularly Imprinted Polymer from CLX1180 via Three Modes of Polymerization for Selective Adsorption of Glutathione

Jun Zhang,[§] Meng Wang,[§] Wenli Peng, Zhengcan Chen, and Zhenbin Chen*

Cite This: *ACS Omega* 2020, 5, 13777−13784

Read Online

ACCESS | Metrics & More | Article Recommendations | Supporting Information

ABSTRACT: A novel glutathione (GSH) surface molecularly imprinted polymer (SMIP) was prepared using modified macroporous adsorption resin (MAR) CLX1180 as a solid substrate, glutathione as a template, acrylamide (AM) and *N*-vinyl pyrrolidone (NVP) as functional monomers, and *N*,*N*′-methylenebisacrylamide (NMBA) as a cross-linker. The reaction could be initiated by three different ways, using CLX1180, GSH, and both, which was proved by the experimentation. The morphology and structure of this polymer were characterized by scanning electron microscopy (SEM), Fourier transform infrared (FTIR) spectroscopy, and time-of-flight mass spectrometry (TOF-MS). The maximum adsorption capacity of GSH approached 39.03 mg·g^{-1}, and the separation degree related to L-cysteine was as high as 4.18. Pseudo-first-order and Langmuir models were well fitting the adsorption properties. GSH-SMIP could be used for three adsorption/desorption cycles with only a slight decrease of adsorption capacity.

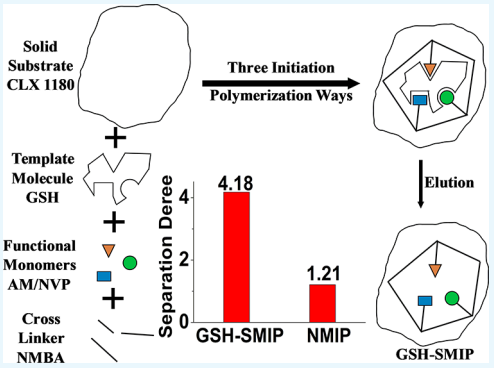

1. INTRODUCTION

Glutathione (GSH) is a type of water-soluble, high value-added compound containing amino acid residues of glutamate, glycine, and cysteine sequentially.[1] Due to its various physiological functions, such as detoxification, radioprotection, antiallergic, liver protection, and antioxidant defense, GSH is extensively used in pharmaceutical, food, cosmetics, and other industries.[2] Chemical synthesis[3] and extraction from animals, plants, and microorganisms[4] are two alternative routes to obtain GSH. Compared to chemical synthesis, extraction is more attractive due to its environmental friendliness and the abundance of relevant natural resources. Unfortunately, methods for the separation and enrichment of GSH—extraction, salting out, ion exchange, concentration, or crystallization[5]—can lead to problems such as environmental pollution and high cost.[6] Therefore, it is necessary to find a more efficient and low-cost method for the separation and enrichment of GSH.

Surface molecular imprinting technology (SMIT) is an attractive method for adsorbent preparation.[7] The preparation method of surface molecularly imprinted polymers (SMIPs) has characteristics different from other traditional adsorption methods: it is easy to obtain molecularly imprinting recognition sites,[8] fast diffusion mobility,[9] and good dynamic performance.[10] In addition, nonspecific adsorption[11] and the embedding phenomenon of the molecularly imprinting recognition sites of the SMIP are decreased.[12] However, SMIPs about GSH are scarcely reported at present and the selectivity is still not high, limiting their scope of application. Macroporous adsorption resin (MAR) is one of the most applied substrate materials because it has many advantages, such as greater specific area and larger pore size distribution, physical and chemical stability, certain adsorption selectivity, and diversity in structure and functional groups.[13] Therefore, this study presents a simple and convenient one-pot method for the synthesis of surface molecularly imprinted polymers for glutathione (GSH-SMIPs), which uses modified macroporous adsorption resin (MAR), CLX1180 as a solid substrate, GSH as a template molecule, acrylamide (AM) and *N*-vinyl pyrrolidone (NVP) as functional monomers, and *N*,*N*′-methylenebisacrylamide (NMBA) as a cross-linker. It is generally recognized that this kind of polymerization, going through physical adsorption−nucleophilic substitution of ions, initiates a reaction.[14] This intriguing experimental phenomenon shows that this reaction could initiate polymerization in three different ways: CLX1180, GSH, and both. The special mechanism of initiation was studied in detail. GSH-SMIP was used as an SMIT adsorbent for the separation and extraction of GSH from L-cysteine (L-cy) by liquid chromatography because

Received: March 1, 2020
Accepted: May 25, 2020
Published: June 3, 2020

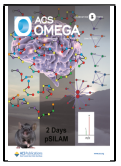

ACS Publications

© 2020 American Chemical Society

L-cy is one component of GSH, while its molecular size is smaller than that of GSH, making L-cy a meaningful contrasting molecule for separation.[15] The adsorption selectivity of our SMIPs is much higher than that of other SMIPs.[16−19] Additionally, the characterization, adsorption kinetics, isotherms, and reusability were investigated in detail. Particularly, we present and discuss the impact of the interaction between the functional monomer and template molecules represented by adsorption behaviors.

2. RESULTS AND DISCUSSION

The scanning electron microscopy (SEM) images of GSH-SMIP and nonmolecularly imprinted polymer (NMIP) are shown in Figure 1. It shows that there was an obvious

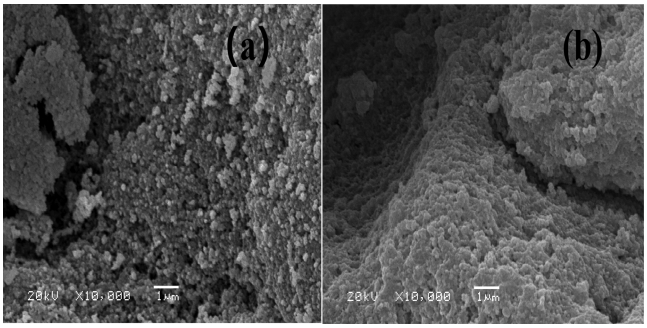

Figure 1. Images of (a) GSH-SMIP and (b) NMIP.

difference in the surface morphology structure between them, that is, the surface of NMIP was smooth and compact, while that of GSH-SMIP was rougher.

The Fourier transform infrared (FTIR) spectra of LX1180 and CLX1180 are shown in Figure S1. It was found that two characteristic absorption peaks of $-CH_2Cl$ occurred at 1270 and 668 cm^{-1}, which indicated that $-CH_2Cl$ had been introduced successfully. Simultaneously, the crest of the absorption peak at 994 cm^{-1} of LX1180 shifted to 971 cm^{-1} and the relative intensity at a frequency of 1378 cm^{-1} of CLX1180 increased obviously. These changes were caused by the introduction of $-CH_2Cl$, which ultimately resulted in the change of the molecular structure of LX1180 after chloromethylation.[20]

The FTIR spectra of CLX1180, NMIP, and GSH-SMIP are shown in Figure 2. It was notable that the strong absorption peak of stretching vibration of C═O of GSH-SMIP was at 1712 cm^{-1}, which indicated that the polymer was synthesized on the surface of CLX1180.[21] The strong absorption peak of the bending vibration of N−H was at 1512 cm^{-1}, and the wide peak at 3446 cm^{-1} was stretching vibration of N−H of GSH-SMIP.[22] As for NMIP and GSH-SMIP, compared to CLX1180, the absorption intensity of the peak 1442 cm^{-1} decreased obviously, while that of the peak 1391 cm^{-1} increased, which demonstrated that the amount of methylene increased and implied that the polymer was synthesized on the surface of CLX1180 significantly.[23] The stretching vibration of C−N−C at the peak 1048 cm^{-1} indicated that NMBA and NVP reacted on the surface of CLX1180.[24]

Some fragment peaks of the following compounds in the time-of-flight mass spectra (TOF-MS) during a polymerization reaction of GSH-SMIP were obtained: 3-isopropoxy alanine, 3-butanone, and 4-hydroxy (Table S1). AM reacted with GSH to form an −NHCO− intermediate, which could be assigned to

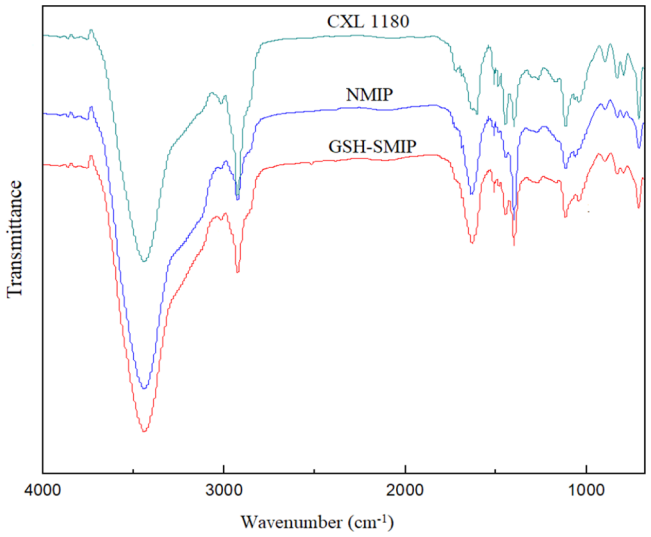

Figure 2. FTIR spectra of GSH-SMIP, NMIP, and CLX1180.

the 3-isopropoxy alanine fragment peaks. NVP and NMBA were cross-linked to generate a C ═ O structure in the product, which could be attributed to the fragment peaks of 3-butanone and 4-hydroxy. This showed that AM, NVP, GSH, and NMBA all participated in the polymerization process.

The polymerization mechanism is shown in Scheme 1. Path 1 shows that CLX1180 was decomposed to produce carbocation, which can attack the double bonds of NMBA, in turn initiating polymerization. In path 2, GSH acts as a natural electron donor, providing electrons and generating oxidized L-glutathione (GSSH). The provided electrons combine directly with NMBA to form ionic free radicals, which then initiate polymerization. In path 3, the electrons provided by GSH combine with RCH_2-Cl to form anion radicals, which then initiate polymerization.

To confirm these three reaction mechanisms, Table 1 and Figure S2 demonstrate the following initiation experiments. It is clearly seen that in term 0, the solution was clear when only NMBA was added. When the temperature was increased to 30 °C, the solution was still clear. In terms 1 to 4, the solutions were not reacted. This infers that GSH or CLX1180 could not initiate AM or NVP polymerization. The reaction of CLX1180 and NMBA could not be initiated at 4 °C, but after increasing the temperature to 30 °C, a white gel was obtained (terms 5 and 10). After the conditions were controlled as in term 10, benzyl chloride was conscripted to instead CLX1180, and the white gel was also obtained (term 11). Obviously, because of the induced effect, carbocation of benzyl chloride or CLX1180 attacking unsaturated bonds initiated polymerization.[25] This was due to heating leading to energy increase; when it exceeds activation energy, polymerization will happen. In terms 6 and 7, we could observe white turbidity in the tubes, because vitamin C (Vc) was an electron donor, which could initiate NMBA polymerization like GSH.[26] It is worth mentioning that after increasing the temperature from 4 to 30 °C, the amounts of the white turbidity reduced and the solution turned slightly viscous (term 9). Therefore, GSH could provide electrons to combine directly with NMBA to form ionic free radicals and then initiate polymerization. In terms 8 and 11, GSH, CLX1180, and NMBA were added into the tubes, and we could see white floe (4 °C) and white gel (30 °C). The same phenomenon was observed in term 13 (benzyl chloride instead

https://dx.doi.org/10.1021/acsomega.0c00926
ACS Omega 2020, 5, 13777−13784

Scheme 1. Polymerization Mechanism of GSH-SMIP

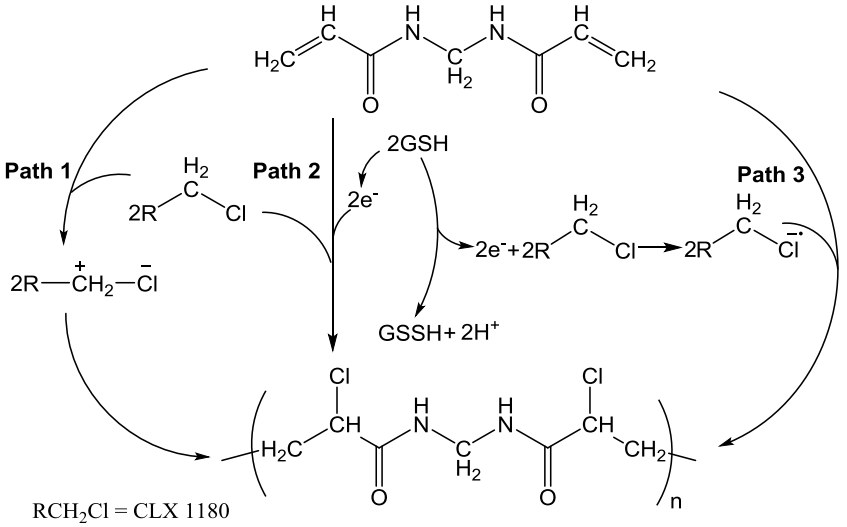

Table 1. Discussion of NMBA Polymerization Mechanism

term	reaction conditions	composition	phenomenon
0	nitrogen atmosphere and standing for 24 h at 4 °C. Then, rising the temperature to 30 °C for 24 h	NMBA	clear
1		GSH and NVP	clear
2		CLX1180 and NVP	clear
3		GSH and AM	clear
4		CLX1180 and AM	clear
5	nitrogen atmosphere and standing for 24 h at 4 °C	CLX1180 and NMBA	clear
6		GSH and NMBA	slightly white turbidity
7		Vc and NMBA	slightly white turbidity
8		GSH, CLX1180, and NMBA	lot of white floe
9	nitrogen atmosphere and stirring for 24 h at 30 °C	GSH and NMBA	white gel
10		CLX1180 and NMBA	white gel
11		benzyl chloride and NMBA	white gel
12		GSH, CLX1180, and NMBA	white gel
13		GSH, benzyl chloride, and NMBA	white gel

of CLX1180). The electrons provided by GSH were combined with benzyl chloride to form anion radicals for polymerization.[27] To further verify the mechanism, we added 2,2,6,6-tetramethylpiperidine-1-oxyl (TEMPO) into GSH, CLX1180, and NMBA under a nitrogen atmosphere and allowed to stand for 24 h at 4 °C, and the reaction phenomenon of the solution was still clear (Figure S3). This explains the free radicals created by GSH, which was captured by the radical scavenger, TEMPO. Therefore, GSH and CLX1180 initiated polymerization via physical adsorption−nucleophilic substitution by active anion radicals.

The relationship between adsorption amount (q) and adsorption time (t) is shown in Figure S4. As can be seen from the figure, q increases with the increase of t and reaches the adsorption equilibrium after 200 min. Figure 3 shows that the pseudo-first-order kinetic model (R^2 = 0.957) is more adaptive to the adsorption behavior of GSH-SMIP than the pseudo-second-order kinetic model (R^2 = 0.910). The adsorption kinetics model of GSH-SMIP was controlled by diffusion. The adsorption capacity of GSH-SMIP was strong by high surface energy, which, due to it having a large number of molecules, imprinted holes in its surfaces and shallows. During the adsorption process, with the increase of time, the adsorption speed became slow, because of the steric effect,

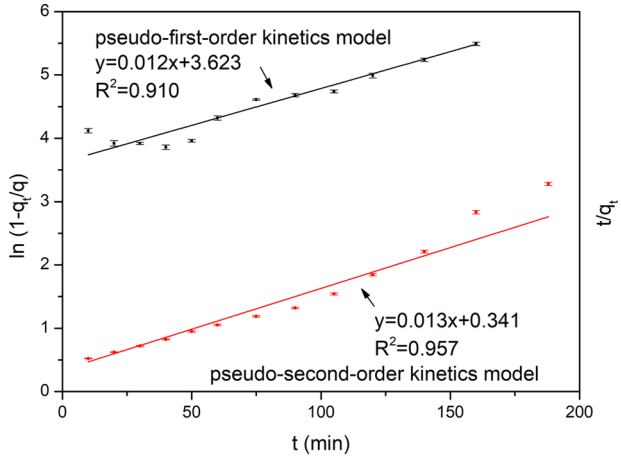

Figure 3. Fitting of pseudo-first-order and pseudo-second-order kinetics models.

which made it more difficult to get the template molecules that had diffused from the surfaces to the deep layers. The template molecules of GSH interact with the functional monomers mainly by hydrogen bond force. Oxygen atoms of carbonyl and hydroxyl of GSH are highly electronegative, which can attract

https://dx.doi.org/10.1021/acsomega.0c00926
ACS Omega 2020, 5, 13777−13784

electrons. The nitrogen atoms of amino of AM have a lone pair of electrons, which can form hydrogen bonds with the carbonyl and hydroxyl groups of GSH. The sulfydryl group of GSH is similar to the highly electronegative hydroxyl group, which can also form hydrogen bonds with AM. Similarly, it can form hydrogen bonds between the amino group of GSH and the carbonyl group of NVP. It is worth noting that although the steric effect was the only factor conforming to the pseudo-first-order kinetic model, R^2 (0.957) was not close to an ideal value (≥0.99). This was because specific recognition due to the specific holes of molecularly imprinting formation influenced the kinetic model results rather than the simple diffusion-controlled adsorption.

As shown in Table 2, it was observed that GSH-SMIP exhibited a higher adsorption capacity toward GSH (39.03 mg·g^{-1}) than that of the control L-cy (9.34 mg·g^{-1}), and the separation degree reached 4.18. The adsorption isotherms of GSH-SMIP are shown in Figures 4 and S5.

Table 2. Separation Degree and Relative Selectivity Degree of GSH-SMIP and NMIP toward GSH and L-cy at 4 °C

	GSH-SMIP		NMIP	
adsorbents	Q (mg·g^{-1})	D	Q (mg·g^{-1})	D
GSH	39.03		10.42	
L-cy	9.34	4.18	8.61	1.21

The adsorption amount (Q) of GSH increases with the increase of the concentration of the original adsorption solution, and the growth rate of Q was fast in the range of 0.1−0.6 g·L^{-1}. After the concentration reached 0.6 g·L^{-1}, the increase rate of Q slowed down. The Freundlich model (R^2 = 0.994) has better fitting results, which indicated that the adsorption behavior of GSH-SMIP was multilayer adsorption. Since the polymerization reaction was exothermic, the local temperature was too high to destroy the self-assembly between the functional monomer and the template molecule, and the imprinted pores and the imperfect imprinted pores in GSH-SMIP would coexist, which will result in a multilayer adsorption characteristic of GSH-SMIP. When the concentration was moderate (0.72−2.4 g·L^{-1}), the linear relationship of Langmuir fitting was good (R^2 = 0.982), which indicated that there were a large number of perfect imprinted pores in GSH-SMIP.

Selectivity experiments were performed using L-cy as the control compound. GSH-SMIP exhibited desirable binding selectivity for GSH. The separation degree and adsorption capacity of GSH-SMIP for GSH were higher than those of NMIP. Hence, the specific recognition for GSH and L-cy of GSH-SMIP determined separation degree (D) to be 4.18. However, the separation degree of NMIP was 1.21, which verified that NMIP showed a lack of specific recognition because no imprinted cavities and recognition sites were generated during polymerization. As shown in Figure 5, it could be seen that GSH-SMIPs were stable, because after three adsorption/desorption cycles, there was only a slight decrease of adsorption capacity.

The maximum adsorption capacity (Q) and separation degree (D) of GSH-SMIP were compared to the adsorption results using several adsorbents, as described in Table 3. The obtained Q and D values of GSH were greater than those reported for other adsorbents. Although some adsorbents presented Q or D values higher than GSH, they had various operation restrictions such as complex synthetic processes and expensive synthesis methods. GSH-SMIP not only had a high adsorption capacity and separation degree, but was also synthesized using a simple one-pot method, so it actually has potential for industrial production.

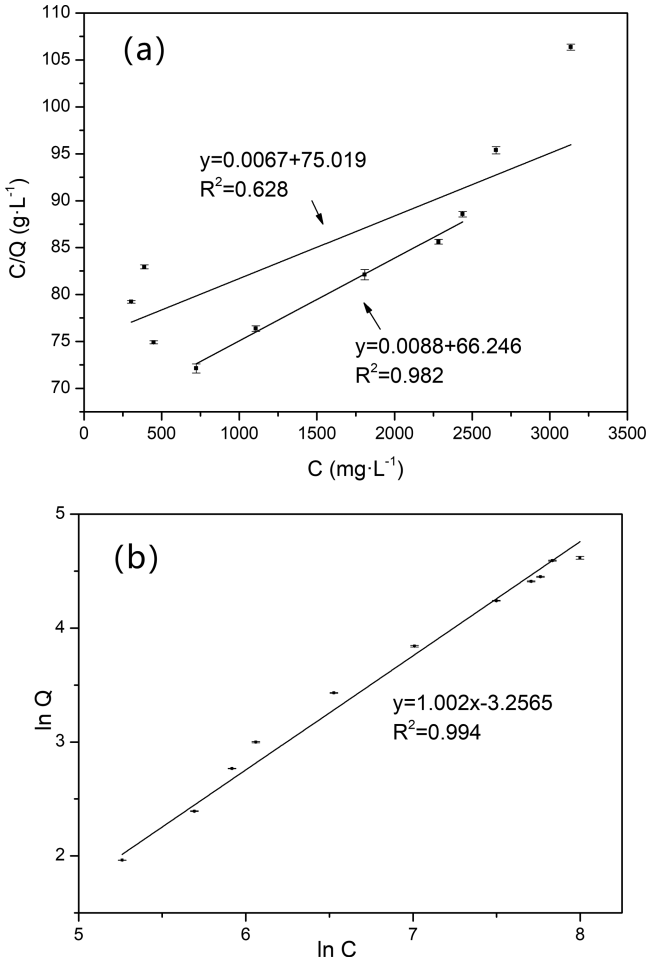

Figure 4. Adsorption isotherms: (a) Langmuir model and (b) Freundlich model.

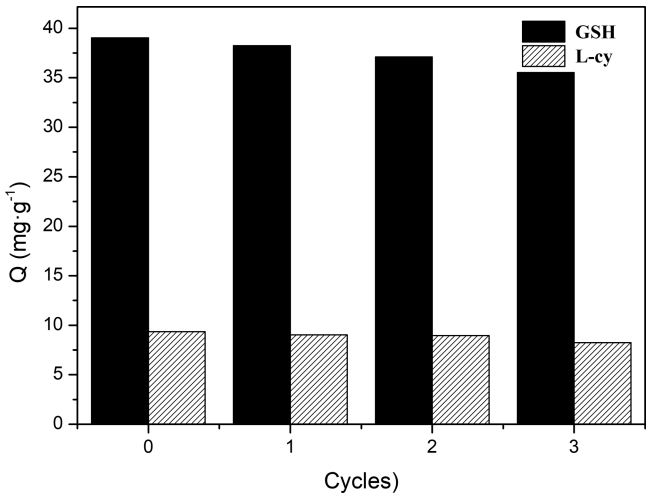

Figure 5. Reusability of GSH-SMIP for three cycles.

https://dx.doi.org/10.1021/acsomega.0c00926
ACS Omega 2020, 5, 13777−13784

Table 3. GSH Maximum Adsorption Capacities and Separation Degree of the Reported Adsorbents in the Literature

adsorbent	adsorbate[a]	Q ($mg·g^{-1}$)	D	ref
iniferter-controlled living radical precipitation polymerization MIP	GSH	10.60		
	Gly-Gly	3.89	2.72	
traditional free-radical precipitation polymerization MIP	GSH	7.11		
	Gly-Gly	3.80	1.87	16
porous imprinted layers MIP	GSH	24.69		
	GSSH	11.34	2.18	
	Gly-Gly	3.71	6.65	17
glutathione-imprinted polymers on fibrous SiO_2 microspheres	GSH	80.8		
	Cys	26.5	3.05	
	Gly-Gly-Gly	26.5	3.05	
	GSSH	44.2	1.83	
	Glu	17.0	4.75	18
GSH-MIP (GSH-SMIP without CXL 1180)	GSH	27		previous work
	L-cy	9.5	2.84	19
GSH-SMIP	GSH	39.03		this work
	L-cy	9.34	4.18	

[a]Abbreviation: glycylglycine (Gly-Gly), cysteine (Cys), glycyl-glycyl-glycine (Gly-Gly-Gly), glutamate (Glu).

3. CONCLUSIONS

In conclusion, glutathione surface molecularly imprinted polymer was employed for initiating by CLX1180, GSH, and both. The absorption time of GSH-SMIP was 200 min in absorbing GSH. The maximum adsorption capacity of GSH was 39.03 $mg·g^{-1}$, and the separation degree was 4.18. The pseudo-first-order and Langmuir models well fit these adsorption properties.

4. EXPERIMENTAL SECTION

4.1. Materials. MAR LX1180 was purchased from Xi'an Sunresin Technology Co., Ltd., Shanxi, China. Glutathione (GSH) and L-cystine (L-cy) were provided by Shanxi Sciphar Biotechnology Co., Ltd., Shanxi, China. *N*-vinypyrrolidone (NVP, CP, Boai Nky Pharmaceuticals Co., Ltd. Henan, China) was distilled at a reduced pressure (b.p. 77−78 °C, 2.0 mmHg; during this process, paradioxybenzene, sulfur deposition, and copper powder were used) to remove the inhibitor. Acrylamide (AM, AR, Kermel Chemical Reagent Company, Tianjin, China) was recrystallized in acetone before use; *N*,*N*′-methylenebisacrylamide (NMBA, AR, Zhongtai Chemical Reagent Company, Shanghai, China) was recrystallized in 66% methanol at 50 °C and dried at a low temperature; analytical-grade potassium dihydrogen phosphate (KH_2PO_4), sodium heptane-1-sulfonate ($C_7H_{15}NaO_3S$), phosphoric acid (H_3PO_4), methanol (MA), ethyl alcohol (EA), tetrachloromethane (CCl_4), potassium nitrate (KNO_3), sodium hydroxide (NaOH), silver nitrate ($AgNO_3$), and ethanoic acid ($C_2H_4O_2$) were purchased from Xi'an Chemical Reagent Factory, Shanxi, China; monochloromethyl ether (ME) was chemically graded as pure and obtained from Puyang Putian Chemical Co., Ltd., Anhui, China; 2,2,6,6-tetramethylpiperidine-1-oxyl (TEMPO) was purchased from Aladdin Co., Ltd., Shanghai, China; analytical-grade anhydrous zinc chloride ($ZnCl_2$) and sodium chloride (NaCl) were purchased from Xi'an Chemical Reagent Factory, Shanxi, China, which were pretreated before use; and secondary distilled water was provided by our lab.

4.2. Preparation of Chloromethylated LX1180 (CLX1180). Chloromethylation of MAR LX1180 was performed according to previous reports.[28,29] First, 20.0000 g of activated LX1180 was added into a dry 500 mL three-neck flask, and 76 mL of CCl_4 was added. Then, the flask was set to a thermostat water bath of 65 °C for 36 h to swell LX1180 completely. Next, 30 mL of ME was added into the flask dropwise. After that, the flask was set in an ultrasonication instrument, and 48.4200 g of the hybrid catalyst was added to speed up the reaction. After reaction for 36 h, the reactant was filtered, and the obtained MAR was rinsed repeatedly until no precipitation was observed as $AgNO_3$ was dropped into the filtrate.

4.3. Synthesis of GSH-SMIP and NMIP. First, 5.00 mL of a GSH solution (200.00 $mmol·L^{-1}$), 45.00 mL of NMBA (200.00 $mmol·L^{-1}$), methanol/water solution (7:3, v/v), 0.3000 g of AM, and 0.2000 g of NVP were added into a 100 mL three-neck flask with magnetic stirring for 10 min. Next, 5.0000 g of CLX1180 was added followed by nitrogen purging for 15 min and static adsorption for 24 h at 4 °C. The mixture was then immersed in a 30 °C water bath for 24 h. After the reaction, the polymers were washed by water repeatedly until no flocculus appeared. Then, the products were purified by Soxhlet extraction with a mixture of methanol/acetic acid (9:1, v/v), which were dried under vacuum at 40 °C for 24 h to obtain GSH-SMIP. Nonmolecularly imprinted polymer (NMIP) was also prepared as a control under the same conditions.

Nonmolecularly imprinted polymers (NMIP) were prepared under the same conditions as GSH-SMIP but without template GSH addition.

4.4. Characterizations of GSH-SMIP, NMIP, CLX1180, and LX1180. The structures of GSH-SMIP, NMIP, CLX1180, and LX1180 were characterized by Fourier transform infrared (FTIR) spectroscopy (Nicolet NEXUS 670, American Nicolet Corporation, Madison, Wisconsin). The images of GSH-SMIP and NMIP were characterized by a scanning electron microscope (SEM, JSM-5600LV SEM, JEOL, Tokyo, Japan). The mass spectrometry analysis of GSH-SMIP was carried out using a time-of-flight mass spectrometer (TOF, MicroTof Q II, Bruker).

4.5. Adsorption Kinetics. GSH-SMIPs (5.0000 g) were sealed into a 200-mesh 7.6 × 50 mm^2 tea bag, which was then submerged in a flask loaded with 500.00 mL of 700.00 $mg·L^{-1}$ GSH aqueous solution. Then, the flask was kept in a 4 °C refrigerator. The adsorption kinetics was obtained by changing the time from 10 to 260 min. The concentration of raffinate is calculated according to the standard curve of GSH. The adsorption capacity (q) of GSH-SMIP is calculated according to eq 1

$$q = \frac{(C_0 - C_t)}{W} V \tag{1}$$

The pseudo-first-order kinetic equation is given by eq 2

$$\ln(q - q_t) = \ln q - k_1 t \tag{2}$$

The pseudo-second-order kinetic equation is given by eq 3

https://dx.doi.org/10.1021/acsomega.0c00926
ACS Omega 2020, 5, 13777−13784

$$\frac{t}{q_t} = \frac{1}{k_2 q^2} + \frac{1}{q}t \quad (3)$$

where q (mg·g^{-1}) is the total adsorption capacity of GSH-SMIP; C_0 (mg·L^{-1}) is the concentration of GSH in the initial solution; C_t (mg·L^{-1}) is the concentration of GSH in the solution at time t; V (mL) is the volume of the initial solution; W (g) is the mass of GSH-SMIP; t (min) is the time; q_e (mg·g^{-1}) and q_t (mg·g^{-1}) represent the adsorption capacity of GSH-SMIP towards GSH at equilibrium and at time t, respectively; and k_1 and k_2 are the rate constants of the pseudo-first-order and pseudo-second-order models, respectively.

4.6. Adsorption Isotherms. Seal 14 portions of 0.1000 g of GSH-SMIP were placed in a 200-mesh 7.6 × 50 mm^2 tea bag, which was then put into 14 brown reagent bottles loaded with 50.00 mL of GSH aqueous solution, whose initial concentration varied from 100.00 to 1200.00 mg·L^{-1} at an interval of 100.00 mg·L^{-1}. The experiment was performed at 4 °C for 360 min. Then, the concentration of raffinate was calculated according to the standard curve of GSH, The equilibrium adsorption capacity (Q) of GSH-SMIP was calculated according to eq 4

$$Q = \frac{(C_0 - C_e)}{W}V \quad (4)$$

where Q is the equilibrium adsorption capacity (g·mg^{-1}), C_e is the equilibrium concentration (mg·L^{-1}) of GSH solution, V stands for the volume (mL) of the initial solution, and W is the mass (g) of the GSH-SMIP.

The Langmuir and Freundlich isotherms are given by eqs 5 and 6, respectively

$$\frac{C_e}{Q_e} = \frac{1}{Q_m - k_L} + \frac{C_e}{Q_m} \quad (5)$$

$$\ln Q_e = \frac{\ln C_e}{n} + \ln k_F \quad (6)$$

where Q_e (mg·g^{-1}) and C_e (mg·mL^{-1}) are the adsorption capacity and the residual concentrations of GSH in the solution at equilibrium, respectively; Q_m (mg·g^{-1}) is the maximum adsorption capacity of adsorbent at monolayer; k_L (mL·mg^{-1}) is a characteristic constant more suitable to describe a monolayer adsorption, whereas the Freundlich constant k_F can be used to describe a monolayer adsorption and a multilayer adsorption; and n is the Freundlich constant related to temperature.

4.7. Selectivity of Adsorption of GSH-SMIP/NMIP. A tea bag containing 0.1000 g of GSH-SMIP/NMIP was added into a 100 mL conical flask loaded with 100.00 mL of mixed aqueous solution of GSH and L-cy (the concentration of each component was 700.00 mg·L^{-1}), sealed, and adsorbed for 360 min at 4 °C. Then, the tea bag was removed and stood for 10 min until it was nearly dry. The concentration of raffinate was calculated according to the standard curve of GSH and L-cy. The D value of GSH-SMIP/NMIP was calculated according to eq 7

$$D = \frac{Q_{a(GSH)}}{Q_{a(L-cy)}} \quad (7)$$

where D is the separation degree of GSH-SMIP/NMIP to GSH and L-cy, $Q_{a(GSH)}$ is adsorption capacity of GSH (g·mg^{-1}), and $Q_{a(L-cy)}$ is the adsorption capacity of L-cy (g·mg^{-1}).

4.8. Reusability of GSH-SMIP. A tea bag containing 0.1000 g of GSH-SMIP was added into a 50 mL conical flask loaded with 100.00 mL of mixed aqueous solution of GSH and L-cy (the concentration of each component was 100.00 mg·L^{-1}), sealed, and adsorbed for 6 h at 4 °C. Then, the tea bag was removed and stood for 10 min until it was nearly dry. Thereafter, it was transferred into a 100 mL conical flask loaded with 50.00 mL of aqueous solution and desorption for 4 h at 4 °C. Then, the tea bag was removed and stood until it was nearly dry. The above method was repeated for three adsorption/desorption cycles. The concentrations of GSH and L-cy in the raffinate were calculated according to the standard curve of GSH and L-cy. Q_a and Q_e of GSH-SMIP were calculated, respectively, using eqs 8 and 9

$$Q_a = \frac{(C_0 - C_1)}{W}V \quad (8)$$

$$Q_d = \frac{C_d V}{W} \quad (9)$$

where Q_a is the adsorption capacity of GSH and L-cy (mg·g^{-1}), C_0 is the concentration of GSH or L-cy in the initial mixture, C_1 is the concentration of GSH and L-cy in the raffinate after adsorption (mg·L^{-1}), V is the volume of the initial solution (mL), W is the mass of GSH-SMIP (g), Q_d is the desorption capacity of GSH or L-cy (mg·g^{-1}), and C_d is the concentration of GSH or L-cy in the raffinate after desorption (mg·L^{-1}).

4.9. Construction of High-Performance Liquid Chromatography (HPLC) Condition. Different peak areas of the mixture of GSH and L-cy before and after absorption were measured with HPLC. The HPLC analysis was performed in a Hitachi L-2400 series HPLC system (Hitachi Ltd., Tokyo, Japan) equipped with a PM0801 organizer, a PM1110 pump, a PM1210 autosampler, a PM1310 column oven, and a PM1410 UV. The HPLC system was managed by Primaide System Manager D-1000 software. The chromatographic separation of analytes was performed on a SinoChrom ODS-BP C18 analytical column (250 × 4.6 mm^2, i.d., 5 μm). The temperature of the column was maintained at 308.15 K. The flow rate, injection volume, and detection wavelength were set at 1.0000 g·L^{-1}, 20 μL, and 210 nm, respectively. The mobile-phase volume ratio of the aqueous solution of potassium dihydrogen phosphate-sodium (KH_2PO_4), heptane-1-sulfonate ($C_7H_{15}NaO_3S$), and methanol was 97:3 (v/v).

4.10. HPLC Standard Curves of GSH and L-cy. Different concentrations of GSH and L-cy solutions were prepared, and their peak areas were measured with HPLC. The peak area at a given concentration was calculated with at least nine data points, and the relationship between peak area (A) and concentration (C) was plotted as Figure S6. It showed a good linear relationship between A and C (the fitting equation of GSH was $A = 12.36C - 644.39$, $R^2 = 0.9936$, $S = 0.12\%$, $n = 9$) as the concentration was in the range of 300.00−700.00 mg·L^{-1}. The method of preparation of the standard curve of L-cy was the same concentration range as GSH (the fitting equation of L-cy was A = 3.13C + 0.18, R^2 = 0.9941, S = 0.12%, n = 9).

■ ASSOCIATED CONTENT

Supporting Information

The Supporting Information is available free of charge at https://pubs.acs.org/doi/10.1021/acsomega.0c00926.

https://dx.doi.org/10.1021/acsomega.0c00926
ACS Omega 2020, 5, 13777−13784

FTIR spectra of LX1180 and CLX1180 (Figure S1); TOF analysis of GSH-SMIP (Table S1); polymerism of NMBA under different conditions (the test tube numbers were the corresponding Table S2 terms) (Figure S2); phenomenon of polymerism under GSH, CLX1180, and NMBA at nitrogen atmosphere and standing for 24 h at 4 °C added and not added with tempo (Figure S3); relationship of adsorption capacity (q) and adsorption time (t) of GSH-MIP (Figure S4); effect of initial GSH concentration on the adsorption capacity of GSH-MIP (Figure S5); retention times of GSH and L-cy, and standard curves of the relationship between peak area and concentration of GSH and L-cy (Figure S6) (PDF)

AUTHOR INFORMATION

Corresponding Author

Zhenbin Chen − *State Key Laboratory of Advanced Processing and Recycling of Nonferrous Metals and School of Materials Science and Engineering, Lanzhou University of Technology, Lanzhou 730050, Gansu, China*; Email: zhenbinchen@163.com

Authors

Jun Zhang − *State Key Laboratory of Advanced Processing and Recycling of Nonferrous Metals and School of Materials Science and Engineering, Lanzhou University of Technology, Lanzhou 730050, Gansu, China*; orcid.org/0000-0003-2121-4510

Meng Wang − *State Key Laboratory of Advanced Processing and Recycling of Nonferrous Metals and School of Materials Science and Engineering, Lanzhou University of Technology, Lanzhou 730050, Gansu, China*

Wenli Peng − *State Key Laboratory of Advanced Processing and Recycling of Nonferrous Metals and School of Materials Science and Engineering, Lanzhou University of Technology, Lanzhou 730050, Gansu, China*

Zhengcan Chen − *State Key Laboratory of Advanced Processing and Recycling of Nonferrous Metals and School of Materials Science and Engineering, Lanzhou University of Technology, Lanzhou 730050, Gansu, China*

Complete contact information is available at: https://pubs.acs.org/10.1021/acsomega.0c00926

Author Contributions

§J.Z. and M.W. contributed to this work equally.

Notes

The authors declare no competing financial interest.

ACKNOWLEDGMENTS

This work was supported by the National Natural Science Foundation, China (Grant 51061009); Shenyang National Laboratory for Materials Science (18LHZD003); and State Key Laboratory of Advanced Processing and Recycling of Nonferrous Metals (18LHPY004).

REFERENCES

(1) Hu, S. Y.; Nie, Z. Y.; Yuan, Q. S. Research Advance on Reduced Glutathione. *Food Drug* **2009**, *11*, 69−71.

(2) Wierzbicka, G. T.; Hagen, T. M.; Tones, D. P. Glutathione in food. *J. Food Compos. Anal.* **1989**, *2*, 327−337.

(3) Tong, Y. J.; Xin, Y.; Yang, H. L.; Zhang, L.; Zhang, Y. R.; Chen, Y.; Xia, X. L.; Wang, W. Preparation and Performance Research on Glutathione Molecularly Imprinted Polymers. *Chromatographia* **2011**, *74*, 443−450.

(4) Dinçer, A.; Zihnioğlu, F. Preparation of Glutathione Imprinted *Polymer. Prep. Biochem. Biotechnol.* **2010**, *40*, 188−197.

(5) Chen, Y. X.; Gao, B. J.; Jiang, G. M.; Zhang, R. X. Constituting Chiral Caves by Using Novel Surface-Molecular Imprinting Technique and Realizating Chiral Separation of Enantiomers of Amino Acid. *Acta Chim. Sin.* **2011**, *69*, 1705−1714.

(6) Song, R. Y.; Hu, X. L.; Guan, P.; Li, J.; Qian, L. W.; Wang, C. L.; Wang, Q. L. Synthesis of porous molecularly imprinted polymers for selective adsorption of glutathione. *Appl. Surf. Sci.* **2015**, *332*, 159−166.

(7) Szajnecki, Ł.; Gawdzik, B. Studies on sorption of bifenthrin and diazinon insecticides on molecularly imprinted polymers. *Polym. Adv. Technol.* **2019**, *30*, 1595−1604.

(8) Saavedra, L. N. M.; Penido, R. G.; Santos, L. A.; Ramalho, T. C.; Baeta, B. E. L.; Pereira, M. C.; Silva, A. C. Molecularly imprinted polymers for selective adsorption of quinoline: theoretical and experimental studies. *RSC Adv.* **2018**, *8*, 28775−28786.

(9) Masoumi, A.; Hemmati, K.; Ghaemy, M. Recognition and selective adsorption of pesticides by superparamagnetic molecularly imprinted polymer nanospheres. *RSC Adv.* **2016**, *6*, 49401−49410.

(10) Hassan, S.; Sayour, H.; El Azab, W.; Mansour, M. Synthesis and characterization of molecularly imprinted nanoparticle polymers for selective separation of anthracene. *J. Dispersion Sci. Technol.* **2016**, *37*, 1241−1251.

(11) Yang, W. B.; Li, A.; Fan, J.; Yang, L. C.; Zhang, Q. X. Adsorption of Branched Alkylbenzene Sulfonate onto Styrene and Acrylic Ester Resins. *Chemosphere* **2006**, *64*, 984−990.

(12) Chen, Z. B.; Kang, L.; Di, D. L.; Dong, F.; Yu, H. Chloromethylation research of LX-1180 macroporous adsorption resin in ultrasonic environment. *Adv. Mater. Res.* **2011**, *233*−*235*, 2893−2897.

(13) Liu, X.; Chen, Z.; Long, J.; Yu, H.; Du, X.; Zhao, Y.; Liu, J. Preparation and selectivity evaluation of glutathione molecularly imprinted polymers from aqueous media. *Ind. Eng. Chem. Res.* **2014**, *53*, 16082−16090.

(14) Jia, W.; Chen, Z. B.; Zhao, Y. Y.; Ma, S. M.; Di, D. L. Separation and purification of resveratrol from Polygonum cuspidatum by macroporous adsorption resin mixed-bed techology. *Sep. Sci. Technol.* **2020**, 1473−1484.

(15) Cai, X.; Li, J.; Zhang, Z.; Wang, G.; Song, X.; You, J.; Chen, L. Chemodosimeter-based fluorescent detection of L-cysteine after extracted by molecularly imprinted polymers. *Talanta* **2014**, *120*, 297−303.

(16) Song, R.; Hu, X.; Guan, P.; Li, J.; Zhao, N.; Wang, Q. Molecularly imprinted solid-phase extraction of glutathione from urine samples. *Mater. Sci. Eng., C* **2014**, *44*, 69−75.

(17) Song, R.; Hu, X.; Guan, P.; Li, J.; Wang, C.; Wang, Q. Synthesis of porous molecularly imprinted polymers for selective adsorption of glutathione. *Appl. Surf. Sci.* **2015**, *332*, 159−166.

(18) Wang, Y. F.; Zhou, J. J.; Zhang, B. L.; Tian, L.; Ali, Z.; Zhang, Q. Y. Fabrication and characterization of glutathione-imprinted polymers on fibrous SiO_2 microspheres with high specific surface. *Chem. Eng. J.* **2017**, *327*, 932−940.

(19) Liu, X. J.; Chen, Z. B.; Long, J. P.; Yu, H.; Du, X. Y.; Zhao, Y. M.; Liu, J. B. Preparation and Selectivity Evaluation of Glutathione Molecularly Imprinted Polymers from Aqueous Media. *Ind. Eng. Chem. Res.* **2014**, *53*, 16082−16090.

(20) Chen, Z. B.; Long, J.; Kang, L.; Du, X.; Di, D. L.; Liu, J. Modified macroporous adsorption resin (LX1180) used to adsorb flavonoid. *Pigm. Resin Technol.* **2013**, *42*, 374−387.

(21) Sohn, H. L.; Cho, Y. T.; Lee, B. J. Measurement of carboxyl group separated from a thin film copolymerized by low-temperature plasma at atmospheric pressure of C_2H_2 and CO_2. *Key Eng. Mater.* **2006**, *321*−*323*, 1332−1335.

(22) Malik, S.; Maji, S. K.; Banerjee, A.; Nandi, A. K. A synthetic tripeptide as organogelator: elucidation of gelation mechanism. *J. Chem. Soc., Perkin Trans. 2* **2002**, *27*, 1177−1186.

(23) Ramanathan, T.; Fisher, F. T.; And, R. S. R.; Brinson, L. C. Amino-functionalized carbon nanotubes for binding to polymers and biological systems. *Chem. Mater.* **2005**, *17*, 1290−1295.
(24) Meurisse, I.; Ribeiro-Claro, P. J. A.; Teixeira-Dias, J. J. C.; Pouchan, C. Conformational equilibria for 3-methylstyrene: raman and ftir spectra and ab initio calculations. *J. Raman Spectrosc.* **1995**, *26*, 1033−1037.
(25) Pan, R. Z. *Polymer Chemistry*, 5th ed.; Chemical Industry Press: Beijing, 2011; p 179−182.
(26) Marre, M. T.; Albergoni, F. G.; Moroni, A.; Marre, E. Light-induced activation of electrogenic H^+ extrusion and K^+ uptake in elodea densa depends on photosynthesis and is mediated by the plasma membrane H^+ atpase. *J. Exp. Bot.* **1989**, *40*, 343−352.
(27) Cubbon, R. C. P. The free radical and anionic polymerization of some N-substituted maleimides. *Polymer* **1965**, *6*, 419−426.
(28) Huang, J.; Huang, K.; Liu, S.; Luo, Q.; Shi, S. Synthesis Characterization and Adsorption Behavior of Aniline Modified Polystyrene Resin for Phenol in Hexane and Aqueous Solution. *J. Colloid Interface Sci.* **2008**, *317*, 434−441.
(29) Marre, M. T.; Albergoni, F. G.; Moroni, A.; Marre, E. Light-induced Activation of Electrogenic H^+ Extrusion and K^+ Uptake in Elodea densa Depends on Photosynthesis and is Mediated by the Plasma membrane H^+ ATPase. *J. Exp. Bot.* **1989**, *40*, 343−352.

https://dx.doi.org/10.1021/acsomega.0c00926
ACS Omega 2020, 5, 13777−13784